Moisture sensitivity examination of asphalt mixtures using thermodynamic, direct adhesion peel and compacted mixture mechanical tests

Jizhe Zhang (Corresponding author)

PhD Student

Nottingham Transportation Engineering Centre, Department of Civil Engineering

University of Nottingham, University Park, Nottingham NG7 2RD, United Kingdom

Tel: 0086-13964032980; Email: zhangjizhe2001@163.com

Gordon D. Airey

Professor

Nottingham Transportation Engineering Centre, Department of Civil Engineering

University of Nottingham, University Park, Nottingham NG7 2RD, United Kingdom

James Grenfell

Senior Technical Officer

Nottingham Transportation Engineering Centre, Department of Civil Engineering

University of Nottingham, University Park, Nottingham NG7 2RD, United Kingdom

Alex K. Apeagyei

Research Fellow

Nottingham Transportation Engineering Centre, Department of Civil Engineering

University of Nottingham, University Park, Nottingham NG7 2RD, United Kingdom

Abstract: Moisture damage in asphalt mixtures is a complicated mode of pavement distress that results in the loss of stiffness and structural strength of the asphalt pavement layers. This paper evaluated the moisture sensitivity of different aggregate-bitumen combinations through three different approaches: surface energy, peel adhesion and the Saturation Ageing Tensile Stiffness (SATS) tests. In addition, the results obtained from these three tests were compared so as to characterise the relationship between the thermodynamic and the mechanical tests. The surface energy tests showed that the work of adhesion in dry conditions was bitumen type dependent which is in agreement with the peel test. After moisture damage, all of these three tests found that the moisture sensitivity of aggregate-bitumen combinations were mainly aggregate type dependent. Based on the peel test, the moisture absorption and mineralogical compositions of aggregate were considered as two important factors to moisture sensitivity. This phenomenon suggests that in a susceptible asphalt mixture, the effect of aggregate may be more influential than the effect of bitumen. The SATS test and the peel test showed similar moisture sensitivity results demonstrating the good correlation between these two mechanical tests. However, the surface energy tests and the mechanical tests cannot correlate in terms of moisture sensitivity evaluation.

Keywords: asphalt mixture, surface energy, peel test, SATS, moisture damage

1. Introduction

Asphalt mixtures are widely used as pavement construction materials. During their service life, asphalt pavements have to sustain high traffic loads and harsh environmental conditions leading to deterioration with the passage of time. Based on previous research, moisture damage is mainly characterised as the adhesive failure between aggregate and bitumen or bitumen-filler (mastic) [1]. So, it has been suggested that the adhesion between aggregate and bitumen in the

dry condition and its degradation with the presence of water are two main attributes which determine the moisture sensitivity of pavements. The adhesion between aggregate and bitumen can be described by four theories which are chemical bonding theory, electrostatic theory, mechanical theory, and thermodynamic theory [2].

Moisture damage is an extremely complicated mode of asphalt mixture distress that leads to the loss of stiffness and structural strength of the asphalt pavement layers and eventually the costly failure of the road structure [3]. Although not all damage is caused directly by moisture, its presence increases the extent and severity of already existing distresses like cracking, potholes and rutting [4]. The existence of moisture in the pavement can result in the loss of cohesion within the bituminous binder itself or the loss of interfacial adhesion between aggregate and bitumen [5, 6]. The sensitivity of asphalt mixtures to moisture attack has been related to mineralogical compositions of aggregates, surface texture of aggregates, bitumen chemistry and the compatibility between bitumen and aggregate [7, 8]. According to previous research, aggregate which has a porous, slightly rough surface and contains more Ca, Al and Mg exhibits relatively high moisture durability [9], while, bitumen which has more carboxylic acids and sulfoxides and good wettability will bond well with aggregate [10]. Moreover, other studies have demonstrated that the surface energy of the materials control the wettability between bitumen and aggregate [4]. For the well coated aggregate, it is hard for water to penetrate into the aggregate-bitumen interface to break the aggregate-bitumen bond.

As the performance of asphalt mixtures in the presence of water is a complex issue, numerous research studies have been carried out to simulate moisture damage. Testing methods such as the boiling water and immersion tests are used to evaluate the adhesive properties of loose asphalt mixtures [6]. However, these tests only rely on a comparative evaluation so the results cannot be used to explain the actual mechanisms that contribute to moisture damage and it is

hard to correlate test data with field performance. The Indirect Tensile Test [11], Hamburg Wheel Tracking Device [12] and Saturation Ageing Tensile Stiffness (SATS) test [1] are methods which focus on compacted asphalt mixtures to predict their degradation under simulated conditioning. The Pneumatic Adhesion Tensile Testing Instrument (PATTI) and peel tests are used to directly measure the degradation of bonding strength of aggregate-bitumen interfaces [13, 14]. Furthermore, surface free energy properties are considered to represent the physico-chemical surface characteristics of bitumen and aggregates and have been used as a tool for moisture damage evaluation [15, 16]. The surface free energy is defined as the minimum amount of work required for a crack to propagate in an elastic material [17]. These tests have been used to evaluate the moisture sensitivity of asphalt mixtures with most of these only relating moisture damage to mechanical deterioration. However, the physical and chemical properties of aggregate and bitumen are not explained in detail and correlated with the moisture damage evaluation tests. In fact, the physico-chemical properties of aggregate and bitumen play a fundamental role in the generation of moisture damage. The mechanisms of moisture damage in asphalt mixture can be better understood if the physico-chemical properties of the individual material (aggregate and bitumen) are linked to the mechanical distress of the asphalt mixtures. In addition, different moisture damage evaluation methods were performed based on different testing procedures using different specimens but the correlations between these tests are not always well established.

The main aim of this paper is to better understand the influence of moisture on the deterioration of asphalt mixtures. As mentioned above, the main causes of moisture damage in asphalt mixtures are related to the adhesive properties of the aggregate-bitumen interface and its degradation in the presence of water. In the presence of water, the bitumen film is removed from the aggregate surface because of the weak boundary between these two materials. The physical and chemical properties of bitumen and aggregate play an important role in the

bonding strength of the aggregate-bitumen interface. Five different types of aggregate (two limestones and three granites) and two types of bitumen were selected for testing. The fundamental properties of the individual material such as the rheological properties of bitumen, moisture absorption and mineralogical compositions of aggregates were characterised. These fundamental properties of the individual materials can be used to explain the cause of good or poor moisture performance of asphalt mixtures. The surface energy properties of bitumen and aggregates were obtained by using the dynamic contact angle (DCA) and dynamic vapour sorption (DVS) tests, respectively. The surface energy results of different types of bitumen and aggregates were then used to calculate the adhesion between these two materials with and without the presence of water based on thermodynamic theory. In addition, the adhesion properties of the aggregate-bitumen interface and its moisture sensitivity were evaluated by using a direct tension peel test. Furthermore, the moisture sensitivity of compacted asphalt mixtures was measured using the Saturation Ageing Tensile Stiffness (SATS) test. Finally, the correlations of these different tests were analysed by comparing the moisture sensitivity results.

2. Materials

2.1 Bitumen

Two types of bitumen, B1 and B2, from the same crude source, with penetration grades of 40/60 and 70/100 respectively were used in the study. The rheological properties of the bitumen were characterised using softening point (BS EN 1427) and penetration (BS EN 1426) tests. Based on the tests, the softening points of B1 and B2 were 51.2°C and 45.2°C respectively, whereas the measured penetration of B1 at 25°C was 46 (0.1mm) compared with 81 (0.1mm) for B2. These data indicates that the B1 bitumen is stiffer than the B2 bitumen.

2.2 Aggregates

Five aggregates from different quarries were selected as substrates. They included two limestone aggregates (L1 and L2) and three granite aggregates (G1, G2 and G3). In this research, aggregates of L1, L2, G1, G2 and G3 were used to prepare the aggregate substrates and perform the peel test, while aggregates of L1, G1, G2, and G3 were used to prepare compacted asphalt mixtures so as to perform the SATS test. The water absorptions of these five aggregates were evaluated based on the ASTM standard (ASTM C127-15) and the results are shown in Table 1.

The mineralogical compositions of different aggregates were studied using a Mineral Liberation Analyser (MLA). The MLA is a method used to identify the mineral phases of aggregate surfaces by using the combined evaluation of an automated scanning electron microscope (SEM) and multiple energy dispersive X-ray detectors (XRD). The detailed procedures used for the MLA test can be seen in previous publications [13, 18].

The MLA scans and the mineral compositions for the five aggregates are presented in Figure 1. For the limestone (L1 and L2) samples, calcite is the predominant phase when compared to the other minerals present, with 96.98% and 99.48% by weight, respectively. However, granite is made up of a number of different mineral phases. Chlorite, albite and quartz are the common dominant minerals for these three granite aggregates with presences higher than 10%. There are three other minerals, epidote, anorthite and k-feldspar detected in G1, G2 and G3, respectively, with presences higher than 10%. It is believed that the large proportion of the albite and quartz phases have the potential to lead to moisture damage, due to their poor adhesion with bitumen [19].

3. Experimental Programme

3.1 Surface energy evaluation

3.1.1 Surface energy of bitumen

A Cahn Model dynamic contact angle (DCA) analyser was used to measure the contact angles of probe liquids on bitumen coated glass slides under dynamic conditions. This is an indirect contact angle measurement by immersing a plate into a liquid and calculating the angle from the measured force [20].

Three probe liquids including water, glycerol and di-iodomethane were selected and five repeat tests were performed for each probe liquid in this study. During testing, the bitumen-coated glass slides were immersed up to a maximum depth of 5 mm and then withdrawn from the liquid by moving the stage up and down at a constant speed of 40 μm/s. The weight of the slide measured by the microbalance was recorded continuously during the advancing and receding process. After data acquisition, the representative mass-depth line area was manually selected and used to determine the contact angle between the bitumen and the probe liquid [4].

The difference between the weight of a plate measured at different times, (ΔF), recorded by the microbalance was used to calculate the contact angle. The contact angle between the probe liquid and surface of the bitumen-coated slide was calculated from the following equation [21]:

$$\cos\theta = \frac{\Delta F + V_{im}(\rho_L - \rho_{air} g)}{P_t \gamma_L} \quad (1)$$

where P_t is the perimeter of the bitumen-coated plate, γ_L is total surface energy of the probe liquid, ΔF is the difference between weight of plate in air and partially submerged in probe liquid, V_{im} is volume of solid immersed in the liquid, ρ_L is the density of the liquid, ρ_{air} is the air density, and g is the gravitational force.

To obtain surface energy values for the bitumen, contact angle values using the three selected probe liquids were measured and applied to the Young-Dupre equation for the work of adhesion (W_{SL}) between the two materials:

$$W_{SL} = \gamma_L(1 + \cos\theta) = 2\sqrt{\gamma_S^{LW}\gamma_L^{LW}} + 2\sqrt{\gamma_S^-\gamma_L^+} + 2\sqrt{\gamma_S^+\gamma_L^-} \quad (2)$$

where subscripts L and S represent liquid and solid respectively, and θ is the contact angle.

Three equations were thus produced using the known surface energy components of the three probe liquids for the determination of the three energy components ($\gamma^{LW}, \gamma^+, \gamma^-$) of the bitumen.

3.1.2 Surface energy of aggregate

Due to the high surface energy of aggregate materials, it is difficult to use the contact angle technique as probe liquids readily spread on the surface and the contact angles approach to zero. Therefore, a dynamic vapour sorption system (DVS Advantage 2, Surface Measurement Systems, Middlesex, UK) was used to determine the surface energy of the aggregates. By using this approach, the mass of the aggregate increases due to the adsorption of probe vapours at their surfaces and this increased mass was then measured using a sensitive balance.

The specific surface area of the aggregate was calculated by using the Brunauer-Emmett-Teller (BET) approach as shown below [22]:

$$SSA = \left(\frac{n_m N_o}{M}\right)\alpha \quad (3)$$

where SSA is the specific surface area of aggregate (m^2), n_m is the monolayer specific amount of vapour adsorbed on the surface of aggregate (mg), N_o is Avogadro's number (6.022 x 1023

mol^{-1}), M is the molecular weight of the vapour (g/mol) and α is the projected or cross-sectional area of the vapour single molecule (m^2).

The number of vapour molecules adsorbed on the aggregate surface is determined by using the Langmuir approach [22]:

$$\frac{P}{n(P_o-P)} = \left(\frac{c-1}{n_m c}\right)\frac{P}{P_o} + \frac{1}{n_m c} \quad (4)$$

where P is the partial vapour pressure (Pa), P_o is the saturated vapour pressure of solvent (Pa), n is the amount of vapour adsorbed on the surface of the absorbent (mg), and c is the BET constant (a parameter theoretically related to the net molar enthalpy of the adsorption).

The surface energy of aggregate reduced as the vapour molecules adsorbed on its surface. So, spreading pressure as a result of adsorption of the vapour molecules can be expressed as:

$$\pi_e = \gamma_S - \gamma_{SV} \quad (5)$$

where π_e is the spreading pressure at the maximum saturated vapour pressure or equilibrium spreading pressure (mJ/m^2), γ_S is the aggregate surface energy in a vacuum, and γ_{SV} is the aggregate surface energy after exposure to vapour.

Spreading pressure at the maximum saturation vapour pressure for each solvent, π_e, is calculated by using the following Gibbs free energy model [22]:

$$\pi_e = \frac{RT}{A}\int_0^{P_o}\frac{n}{P}dP \quad (6)$$

where R is the universal gas constant (83.14cm^3 bar/mol.K), and T is the absolute temperature (K).

By introducing spreading pressure, π_e, in the Young-Dupre relation (Eq.2), the following relationship is obtained:

$$W_{SL} = \pi_e + \gamma_{LV}(1 + \cos\theta) \quad (7)$$

The contact angle value for high energy solids such as aggregates is zero, therefore, Eq.7 can be re-written as:

$$W_{SL} = \pi_e + 2\gamma_{LV} \quad (8)$$

By substituting the above relation into Eq.2, the following equation is obtained:

$$2\gamma_L + \pi_e = 2\sqrt{\gamma_S^{LW}\gamma_L^{LW}} + 2\sqrt{\gamma_S^+\gamma_L^-} + 2\sqrt{\gamma_S^-\gamma_L^+} \quad (9)$$

Spreading pressures from three probe vapours are measured. Then, the three energy components of the aggregate ($\gamma_S^{LW}, \gamma_S^+, \gamma_S^-$) can be determined by solving three simultaneous equations.

3.1.3 Work of Adhesion and Moisture Sensitivity

After achieving the surface energy parameters of bitumen and aggregate, the dry work of adhesion, the work of debonding in the presence of water and the cohesion of bitumen can be calculated. These three bond energy parameters can then be used to assess the moisture sensitivity of the asphalt mixtures. The work of adhesion between bitumen and aggregate can be calculated by performing surface free energy calculations using equation 10 [18]:

$$W_{12}^a = 2\sqrt{\gamma_1^{LW}\gamma_2^{LW}} + 2\sqrt{\gamma_1^+\gamma_2^-} + 2\sqrt{\gamma_1^-\gamma_2^+} \quad (10)$$

The bitumen work of cohesion is the work done to create a new unit area by fracture in the neat bitumen phase and is twice the total surface energy of the material.

In general case, the work of adhesion (or work of debonding) of two materials in contact with a third medium can be explained by the following equation. It is the reduction in bond strength of an aggregate-bitumen system when water displaces the bitumen from the aggregate surface.

$$W_{132} = -\Delta G^{a}_{132} = \gamma_{13} + \gamma_{23} - \gamma_{12} \quad (11)$$

where subscripts 1, 2 and 3 represent aggregate, bitumen and water, respectively.

When the surface energy parameters of water are entered into Equation 11, the equation can be expanded as follows:

$$W^{a}_{132} = \left\{\left(\left(\sqrt{\gamma_1^{LW}} - 4.67\right)^2\right) + \left(2 \times \left(\sqrt{\gamma_1^{+}} - 5.05\right) \times \left(\sqrt{\gamma_1^{-}} - 5.05\right)\right)\right\} + \left\{\left(\left(\sqrt{\gamma_2^{LW}} - 4.67\right)^2\right) + \left(2 \times \left(\sqrt{\gamma_2^{+}} - 5.05\right) \times \left(\sqrt{\gamma_2^{-}} - 5.05\right)\right)\right\} - \left\{\left(\left(\sqrt{\gamma_2^{LW}} - \sqrt{\gamma_1^{LW}}\right)^2\right) + \left(2 \times \left(\sqrt{\gamma_2^{+}} - \sqrt{\gamma_1^{+}}\right) \times \left(\sqrt{\gamma_2^{-}} - \sqrt{\gamma_1^{-}}\right)\right)\right\} \quad (12)$$

3.2 Peel test

The peel test (as described in ASTM D6862-11) is used to calculate the adhesive fracture energy of flexible laminates and this technique has been widely used in aerospace, automotive and electronics applications [23, 24, 25]. This test is considered to be a reliable method to measure the fracture energy if suitable corrections for plastic work can be performed, as it can be accurately controlled the film thickness, peel speed and temperature [26].

3.2.1 Sample preparation

For the peel test, the specimen should be rectangular, with the rigid aggregate substrate and the flexible peel arm adhered along most of the length. The rigid aggregate should be thick enough to withstand the expected tensile force. The flexible peel arm should have good adhesion with

bitumen to avoid fracture at their interface. In this research, an aluminium alloy with a thickness of 0.2 mm was selected as the flexible peel arm. According to previous research [27], the overall dimensions of the aggregate substrates used in this research were selected as 150 mm × 20 mm × 10 mm. The aggregate substrates were produced from aggregate boulders. The stone boulders were first wet-sawn to get aggregate slabs with a thickness of 10 mm. Then, the aggregate slabs were trimmed to a size of 150 mm long and 20 mm wide, as shown in Figure 2. The substrates were then polished with sand paper (P800, 21.8 μm) to make sure the surface is visibly flat with no saw marks. Then, the polished slices were cleaned using distilled water and dried at room temperature for at least 24 hours.

The aggregate substrates with dimensions of 150 mm × 20 mm × 10 mm were placed in an oven at 150°C for 1 hour. Bitumen is preheated to 150°C for 1 hour prior to making the joint. Then, these hot aggregate substrates were bonded to the aluminium peel arm using hot bitumen as the adhesive layer. The bitumen film thickness is controlled by placing five steel wire spacers with the diameter of 0.25 mm on the aggregate which results in a 0.25 mm film thickness. The detailed procedure can be seen in previous publications [28, 29, 30].

3.2.2 Moisture conditioning

The prepared aggregate-bitumen adhesion specimens were tested under dry conditions or after moisture conditioning. Moisture was introduced into the aggregate-bitumen interface by submerging the prepared specimens in distilled water at 20°C for 7 days or 14 days, as shown in Figure 3. During the conditioning period, moisture reaches the aggregate-bitumen interface and directly attacks the bond. The specimens should be tested within 1 hour after removing them from the water bath.

3.2.3 Fracture energy evaluation

A universal testing machine (UTM) which can supply a constant rate of grip separation was used to measure the tensile force during the peel test. The specimens were attached to a linear bearing using two clamps while the linear bearing was then installed on the UTM. The peel tests were conducted at a controlled temperature of 20 ± 2°C. During testing, the free end of the peel arm was gripped by the UTM fixture and pulled up at a speed of 10 mm/min with the peel angle maintained at 90°, as shown in Figure 4. The tensile force was recorded during the fracture development and the results used to calculate the fracture energy.

Before calculating the fracture energy of the aggregate-bitumen bond, the mechanical properties of the aluminium peel arm need to be determined using the same tensile speed as the peel test. In order to describe the elastic and plastic deformation of the peel arm, the stress-strain curve was fitted with a bi-linear equation [27]. The purpose of the bi-linear curve fit is to get a number of parameters which are used to calculate the fracture energy. The following parameters of the bi-linear model (Eq. 13) for the peel arm were used for the plastic corrections as described in the following equation:

$$\sigma = \sigma_y + \alpha E_1(\varepsilon - \varepsilon_y) \tag{13}$$

where σ_y is yield stress and ε_y is the yield strain, E_1 is the elastic modulus of the peel arm, E_2 is the plastic modulus of the peel arm and α is the ratio of plastic modulus to elastic modulus, E_2/E_1.

The measured stress-strain curve was modelled using the bi-linear model with the parameters gained from the fitting process shown in Table 2. The value of the corrected fracture energy was then calculated using large displacement beam theory.

3.3 Saturation Ageing Tensile Stiffness (SATS) test

The Saturation Ageing Tensile Stiffness (SATS) test is the first test procedure that combines both ageing and moisture damage by conditioning pre-saturated asphalt mixture specimens at an elevated temperature and pressure in the presence of moisture. The SATS procedure involves conditioning five pre-saturated specimens in a pressure vessel under 0.5 MPa air pressure at a temperature of 85°C for a period of 24 hours. The dimensions and specifications of the SATS testing equipment, including the size and spacing of the holes in the perforated trays are detailed in Clause 953 of Volume 1 of the UK Manual of Contract Documents for Highway Works, 2004 [31]. The key features of the SATS test conditioning procedure can be summarised as follows:

1) The unconditioned (initial) indirect tensile stiffness modulus of each asphalt mixture specimen is measured at 20°C using the Nottingham Asphalt Tester (NAT) [32, 33].

2) The dry mass of each specimen is determined by weighing.

3) The specimens are subsequently immersed in distilled water at 20°C and saturated using a residual pressure of between 40 and 70 kPa for 30 min.

4) The wet mass of each specimen is measured, and the percentage saturation of each specimen calculated and referred to as ‘initial saturation’.

5) The SATS pressure vessel is partly filled with a pre-determined amount of distilled water to submerge the bottom specimen while leaving the other four specimens above the water level. The pressure vessel and water are maintained at the target temperature of 85°C for at least 2 hours before introducing the specimens.

6) The saturated asphalt specimens are then placed into the pressure vessel and maintained at the testing conditions with a pressure of 0.5 MPa and temperature of 85°C for 24 hours.

7) After conditioning, the vessel temperature is cooled down to 30°C and pressure is gradually released. Each specimen is then surface dried and weighed in air. The percentage saturation calculated at this stage is referred to as the 'retained saturation'.

8) The specimens are finally brought back to 20°C and the conditioned stiffness modulus measured once more using a NAT.

9) The ratio of the final stiffness modulus/initial stiffness modulus can thus be calculated, and is referred to as the "retained stiffness modulus".

4. Results

4.1 Surface energy results

4.1.1 Surface energy of bitumen

The calculated surface energy results of the two types of bitumen used in this research are presented in Table 3. The results for the B1 bitumen exhibited a comparatively higher total surface energy in comparison with the result for B2 bitumen.

4.1.2 Surface energy of aggregates

Five aggregates, including two limestones and three granites were tested and the results were used to estimate specific surface area (SSA) and spreading pressure from which the surface energy parameters were calculated. The surface energy components and SSA of the five aggregates are shown in Table 4.

Specific surface area for the various aggregates showed large differences depending on aggregate type. It can be seen that the three granite aggregates showed similar SSA values, while the values for limestone are smaller in comparison with the granite.

The results show that surface energy properties vary considerably, in terms of surface energy components as well as total surface energy. The results indicate that the limestone aggregates have slightly higher van de Waals components (over 75 mJ/m^2) than granite aggregates (under 70 mJ/m^2). In contrast, granite aggregates tend to have higher total surface energy in comparison with limestone. Also, the acid-base components showed significant and irregular differences between these five aggregates. The differences can be attributed to different elemental and mineralogical compositions of the aggregates which in turn will influence the strength of the aggregate-bitumen adhesion and its moisture sensitivity.

4.1.3 Work of adhesion and debonding

Work of adhesion results for the various aggregate-bitumen combinations and the work of cohesion results for bitumen calculated from Equation 10 are shown in Table 5. From this table it can be seen that B1 bitumen has higher work of cohesion and work of adhesion results in comparison with B2 bitumen. In terms of the same bitumen, the aggregate also influences the work of adhesion with G3 having the highest values and G2 having the lowest results. It is important to notice the significantly higher value of work of adhesion at the aggregate-bitumen interface compared to the work of cohesion in the bitumen film. Therefore, in the absence of moisture, the dominant failure mode in asphalt mixtures should be cohesive which is in accordance with experience [19].

Work of debonding values of the aggregate-bitumen combinations and bitumen films in the presence of moisture are presented in Table 6. From this table it can be seen that the value of the work of debonding is aggregate type dependent, which suggests that the physico-chemical properties of the aggregates play a fundamental and more significant role in the generation of moisture damage, than the bitumen properties. This observation is in good agreement with previous research studies [27, 34]. In addition, specimens with a positive work of debonding

are considered more stable than those with negative work of debonding. Aggregate-bitumen combinations with bigger work of debonding values are indicative of better moisture resistance. Based on this principle, specimens comprising of aggregate G2 and L2 would be expected to be more stable than the other three mixtures because of their positive work of debonding values. However, L1, G1 and G3 seem to be sensitive to moisture damage due to their negative work of debonding. In terms of the same aggregate, B2 bitumen tends to achieve lower work of debonding values in comparison with B1. So, the B2 bitumen seems more sensitive to moisture damage. The values of work of debonding for bitumen films are much higher than those for aggregate-bitumen interfaces. This means that in the presence of moisture, the failure mechanism tends to transfer from cohesive to adhesive.

4.2 Peel test

4.2.1 Fracture energy calculation

The purpose of the peel test is to measure the fracture energy of the aggregate-bitumen bonds as a function of material type and moisture conditioning time. Results were obtained for four replicate tests performed on each aggregate-bitumen combination. The tensile force was recorded by the UTM during testing and the tensile load versus displacement curve was plotted, as shown in Figure 5. It can be seen that the tensile force remained at a constant value after the initial stage. Normally, at least 50 mm of constant crack propagation region was defined with the average value of the tensile force being calculated. The average tensile force of each sample and the parameters in Table 2 were entered into the Microsoft excel macro IC Peel software to calculate the fracture energy [35].

4.2.2 Fracture energy in dry conditions

Table 7 shows the average fracture energy and test variability (standard deviation) of all specimens before moisture conditioning. From this table it can be seen that in dry conditions, specimens prepared with the same bitumen have almost the same fracture energy, irrespective of which aggregate was used. This is because in dry constions, a cohesive failure occurred within the bulk of the bitumen, as shown in Figure 6. The fracture energy depended on the cohesive bond of the bitumen layer meaning that all aggregates show almost the same fracture energy in the dry condition. In terms of different bitumen, specimens prepared with B2 bitumen have lower fracture energy than those with B1 bitumen. This correlates well with the work of adhesion values calculated from the surface energy of aggregate and bitumen as shown in Section 4.1.3.

4.2.3 Failure behaviour after moisture conditioning

To simulate the effect of moisture on the bonding properties between bitumen and aggregate, the whole specimens were submersed in water at 20°C for 7 days and 14 days. After moisture conditioning, specimens were removed from the water bath and then subjected to the peel test within a few hours.

The loading behaviour and failure surface of two granite samples were selected for analysis, as shown in Figure 7. It can be seen that these samples showed different loading behavior and failure surfaces due to the different moisture sensitivity of aggregates. The sample prepared with B1-G1 (Figure 7(a)) showed a cohesive failure surface after 14 days of moisture conditioning and the tensile load did not show much decrease in comparison with Figure 5. In contrast, the failure surface of B1-G2 is nearly adhesive and the tensile load decreased significantly. It is interesting to see that the tensile load has a strong relationship with the failure surface. Take Figure 7(b) for example, the tensile load value fluctuates according to the proportion of cohesive/adhesive failure area with cohesive failure tending to exhibit a higher

tensile load while adhesive failure results in a lower value. From this figure it can be seen that the tensile load accurately reflects the failure mode.

4.2.4 Retained fracture energy - influence of binder grade

The effect of moisture on the aggregate-bitumen bond strength could be captured using the retained fracture energy percentage. In general, the larger the magnitude of retained fracture energy of a joint, the greater the resistance to failure from applied loading. The retained fracture energy of specimens after 7 days and 14 days moisture conditioning were calculated by dividing the conditioned fracture energy by the dry fracture energy, and the results are shown in Figure 8. As shown in Figure 8, one effect of moisture on aggregate-bitumen bond strength is a reduction in fracture energy with conditioning time. For the five aggregates used in this research, specimens containing the B1 bitumen showed slightly higher retained fracture energy in comparison with those containing B2 bitumen. It is demonstrated that reducing the stiffness of the bitumen resulted in a decrease in moisture damage resistance.

4.2.5 Retained fracture energy - influence of aggregate source

In terms of the same bitumen, different moisture damage performance occurred because of the different aggregate substrates. The significant difference in retained fracture energy results could be explained by the water absorption and mineral compositions of the aggregates. For G1 aggregate, the dominant mineral phases, albite and quartz, are considered to be sensitive to moisture damage. However, because of its lower moisture absorption (0.13%), it is hard for water to diffuse through the aggregate into the aggregate-bitumen interface to weak the bond. The other two granite aggregates (G2 and G3) with normal moisture adsorption values had the lowest retained fracture energy. This is not surprising as both acidic aggregate sources have long histories of very poor moisture damage performance in the field [1]. In terms of the

limestone aggregates (L1 and L2), both showed good moisture resistance due to their dominant mineral phase (calcite) which can form a stable bond with bitumen even in the presence of water. The slightly lower result of L1 could be attributed to its higher water adsorption (2.21%) in comparison with L2 (0.46%). On this basis, it is reasonable to state that the moisture sensitivity of aggregate-bitumen bonds is not only controlled by the mineralogical compositions but the moisture absorption of the aggregate should also be considered.

4.3 Saturation Ageing Tensile Stiffness (SATS) results – moisture sensitivity of asphalt

As L2 is not a commonly used material in pavement construction, so there is no asphalt specimens were produced. So, in this research, SATS tests were carried out on the samples prepared with bitumen B1 and four aggregates (L1, G1, G2 and G3). The retained stiffness modulus was obtained by dividing the conditioned stiffness modulus by the initial stiffness modulus with the results shown in Figure 9. The higher retained stiffness modulus representing better moisture resistance of the asphalt mixture. It can be seen that the results of B1-L1 and B1-G1 maintained a high level with the retained stiffness values over 70%. However, the values of B1-G2 and B1-G3 showed a rapid decline with the retained stiffness finally down below 30%. It is generally accepted if a retained stiffness of less than 60% is achieved, the mixture is considered to be moisture susceptible [5]. Based on this test, L1 and G1 have good moisture resistance while G2 and G3 are moisture susceptible which correlates well with the peel test results.

5. Correlation between different tests

The correlations of the three tests used in this research were evaluated using the data presented above.

Figure 10 plots the retained fracture energy of the peel test (after 14 days moisture conditioning) and SATS retained stiffness (at 40% moisture saturation). The SATS results at 40% moisture saturation have been determined by fitting a linear regression to the data in Figure 9 and calculating the retained stiffness at 40% moisture saturation [18]. In all cases, a higher value of the parameter suggests better resistance to moisture damage. The two tests ranked the mixtures containing L1 and G1 aggregates as generally better than those containing G2 and G3 aggregates. The results show a good correlation between these two mechanical techniques for evaluating moisture sensitivity.

A comparison of peel test retained fracture energy versus the work of debonding obtained from surface energy testing is provided in Figure 11. The data in the red circles represents results that do not correlate with the linear relationship. It can be seen that these two tests showed different rankings in terms of the moisture sensitivity. For instance, B1-G1 is considered to have the best moisture resistance properties based on the peel test. However, B1-G1 has the lowest work of debonding demonstrating its predicted susceptibility to moisture damage. In addition, B1-G2 also yielded misleading results based on these two tests. It can be concluded that for the aggregates considered in this research, the surface energy-based method does not correlate well with the peel test for moisture sensitivity evaluation.

6. Conclusions

The following conclusions were reached based on the results presented in this study:

- Surface energy parameters of bitumen and aggregates were obtained from the DCA and DVS test, respectively. According to the surface energy-based principles, bitumen properties control the bonding strength of aggregate-bitumen combinations in the dry condition as the work of cohesion is much lower than the work of adhesion.

- The magnitude of the work of debonding in the presence of water was found to be aggregate type dependent rather than bitumen dependent. It is demonstrated that the physico-chemical properties of aggregates play a fundamental and more significant role in the development of moisture damage than bitumen.

- The peel test used in this study was found to be effective in characterising the moisture resistance of the aggregate-bitumen system. The tensile load accurately correlated with the failure mechanisms.

- The retained fracture energy results were shown to be sensitive to moisture conditioning and the moisture resistance could be explained by the moisture adsorption and mineralogical compositions of the aggregates. Limestone tends to have better resistance to moisture damage than granite with the same moisture adsorption. Furthermore, in terms of similar mineralogical compositions, lower moisture adsorption may result in better moisture resistance.

- Retained stiffness values obtained from the SATS tests for B1-L1 and B1-G1 asphalt mixtures were comparatively higher than that for B1-G2 and B1-G3 mixtures. Higher retained stiffness indicates better moisture resistance. The SATS test results appear to be in agreement with the peel test results.

- The peel test and the standard SATS test shows similar ranking in terms of the moisture damage evaluation demonstrating that these two tests correlated well in terms of moisture damage evaluation.

- The surface energy-based tests and peel test showed a different moisture sensitivity results. This demonstrated that the surface energy test cannot correlated with the mechanical tests in terms of moisture damage evaluation.

References

1. Fromm H.J. The mechanisms of asphalt stripping from aggregates surfaces. Journal of the Association of Asphalt Paving Technologists, 1974; 43: 191-223.
2. Bhasin A. Development of Methods to Quantify Bitumen-Aggregate Adhesion and Loss of Adhesion due to Water: PhD dissertation, Texas A&M University, USA. 2006.
3. Airey G.D., Collop A.C., Zoorob S.E. and Elliott R.C. The influence of aggregate, filler and bitumen on asphalt mixture moisture damage. Construction and Building Materials 2008, 22(9): 2015-2024.
4. Grenfell J., Ahmad N., Liu Y., Apeagyei A., Large D. and Airey G.D. Assessing asphalt mixture moisture susceptibility through intrinsic adhesion, bitumen stripping and mechanical damage. Road Materials and Pavement Design 2014, 15(1): 131-152.
5. Airey G.D. and Choi Y.K. State of the Art Report on Moisture Sensitivity Test Methods for Bituminous Pavement Materials. Road Materials and Pavement Design 2002, 3(4): 355-372.
6. Liu Y., Apeagyei A.K., Ahmad N., Grenfell J. and Airey G.D. Examination of moisture sensitivity of aggregate–bitumen bonding strength using loose asphalt mixture and physico-chemical surface energy property tests. International Journal of Pavement Engineering 2014, 15(7): 657-670.
7. Terrel R.L. and Al-Swailmi S. Water sensitivity of asphalt-aggregate mixes: Test selection. SHRPA-403, strategic highway research program. Washington, DC: National Research Council 1994.
8. Abo-Qudais S. and Al-Shweily H. Effect of aggregate properties on asphalt mixtures stripping and creep behaviour. Construction and Building Materials 2007, 21(9): 1886–1898.

9. Bagampadde U., Isacsson U. and Kiggundu B.M. Classical and Contemporary Aspects of Stripping in Bituminous Mixes, Road Materials and Pavement Design 2004; 5(1): 7-43.

10. Petersen J.C. and Plancher H. Model Studies and Interpretive Review and the Competitive Adsorption and Water Displacement of Petroleum Asphalt Chemical Functionalities on Mineral Aggregate Surfaces, Petroleum Science and Technology 1998; 16(1-2): 89-131.

11. Lottman R.P. Predicting Moisture-Induced Damage to Asphaltic Concrete Field Evaluation, NCHRP 246, 1982.

12. Aschenbrener T. Evaluation of Hamburg wheel-tracking device to predict moisture damage in hot-mix asphalt. Transport Research Record 1995; 1492: 193-201.

13. Zhang J., Apeagyei A.K. and Airey G.D. Effect of Aggregate Composition on Moisture Sensitivity of Aggregate-Bitumen Bonds, Transportation Research Board 94th Annual Meeting. 2015 (15-0999).

14. Kanitpong K. and Bahia H.U. Role of adhesion and thin film tackiness of asphalt binders in moisture damage of HMA. Journal of the Association of Asphalt Paving Technologists, 2003, 72: 611-642.

15. Cheng D., Little D.N., Lytton R.L. and Holste J.C. Surface energy measurement of asphalt and its application to predicting fatigue and healing in asphalt mixtures. Transportation Research Record: Journal of the Transportation Research Board 2002; 1810: 44–53.

16. Little D.N. and Bhasin A. Using surface energy measurements to select materials for asphalt pavement. NCHRP Project 9-37, Transportation Research Board, Washington DC, 2006.

17. Griffith A.A., The Phenomena of Rupture and Flow in Solids, philosophical Transactions of the Royal Society of London. Series A, Containing Papers of a Mathematical or Physical Character 1921; 221: 163-198.

18. Grenfell J., Ahmad N., Airey G., Collop A. and Elliott R. Optimising the moisture durability SATS conditioning parameters for universal asphalt mixture application. International Journal of Pavement Engineering 2012; 13(5): 433-450.

19. Apeagyei A.K., Grenfell J. and Airey G.D. Moisture-induced strength degradation of aggregate–asphalt mastic bonds. Road Materials and Pavement Design 2014; 15(1): 239-262.

20. Adamson A.W. and Gast A.P. Physical chemistry of surfaces, 6th Ed., Wiley, New York 1997.

21. Bhasin A. Development of methods to quantify bitumen-aggregate adhesion and loss of adhesion due to water (PhD dissertation). Texas A&M University, College Station, Texas, USA 2006.

22. Ahmad N. Asphalt Mixture Moisture Sensitivity Evaluation using Surface Energy Parameters, PhD Thesis University of Nottingham, March 2011.

23. Kawashita L.F., Moore D.R. and Williams J.G. Analysis of peel arm curvature for the determination of fracture toughness in metal-polymer laminates. Journal of materials science 2005; 40(17): 4541-4548.

24. Horgnies M., Willieme P. and Gabet O. Influence of the surface properties of concrete on the adhesion of coating: Characterization of the interface by peel test and FT-IR spectroscopy. Progress in Organic Coatings 2011; 72(3): 360-379.

25. Leforestier E., Darque-Ceretti E., Peiti D. and Bolla M. Peeling and characterisation of the carbon fibre-based radicular adhesive anchorage interface, International Journal of Adhesion and Adhesives 2007; 27(8): 629–635.

26. Horgnies M., Darque-Ceretti E., Fezai H. and Felder E. Influence of the interfacial composition on the adhesion between aggregates and bitumen: Investigations by EDX,

XPS and peel tests. International Journal of Adhesion and Adhesives 2011; 31(5): 238–247.

27. Blackman B.R.K., Cui S., Kinloch A.J. and Taylor A.C. The development of a novel test method to assess the durability of asphalt road-pavement materials. International Journal of Adhesion and Adhesives 2013; 42: 1-10.

28. Ahmad N., Cui S., Blackman B.R.K., Taylor A.C., Kinloch A.J. and Airey G.D. Predicting Moisture Damage Performance of Asphalt Mixtures. Nottingham Transportation Engineering Centre Report 2011, Report Number: 11091.

29. Zhang J., Airey G.D. and Grenfell J.R.A. Experimental evaluation of cohesive and adhesive bond strength and fracture energy of bitumen-aggregate systems [J]. Materials and Structures, 2015: 1-15.

30. Zhang J., Apeagyei A.K., Airey G.D. and Grenfell J.R.A. Influence of aggregate mineralogical composition on water resistance of aggregate–bitumen adhesion [J]. International Journal of Adhesion and Adhesives, 2015, 62: 45-54.

31. The Highways Agency. Manual of contract documents for highway works, vol. 1, Specification for highway works, Clause 953: durability of bituminous materials – Saturation Ageing Tensile Stiffness (SATS) Test, Highways Agency, Series 900; November 2004.

32. Cooper K.E., and Brown S.F.. Developments of a simple apparatus for the measurement of the mechanical properties of asphalt mixes.In: Proceedings of the eurobitume symposium, Madrid; 1989. P: 494–8.

33. British Standards Institution, Method for determination of the indirect tensile stiffness modulus of bituminous mixtures, BS DD 213; 1993.

34. Apeagyei A.K., Grenfell J. and Airey G.D. Influence of aggregate absorption and diffusion properties on moisture damage in asphalt mixtures. Road Materials and Pavement Design 2015, 16: 404-422.

35. IC Peel software. http://www3.imperical.ac.uk/meadhesion/testprotocols/peel. Imperial College London. Assessed 14 March 2013.

Figures

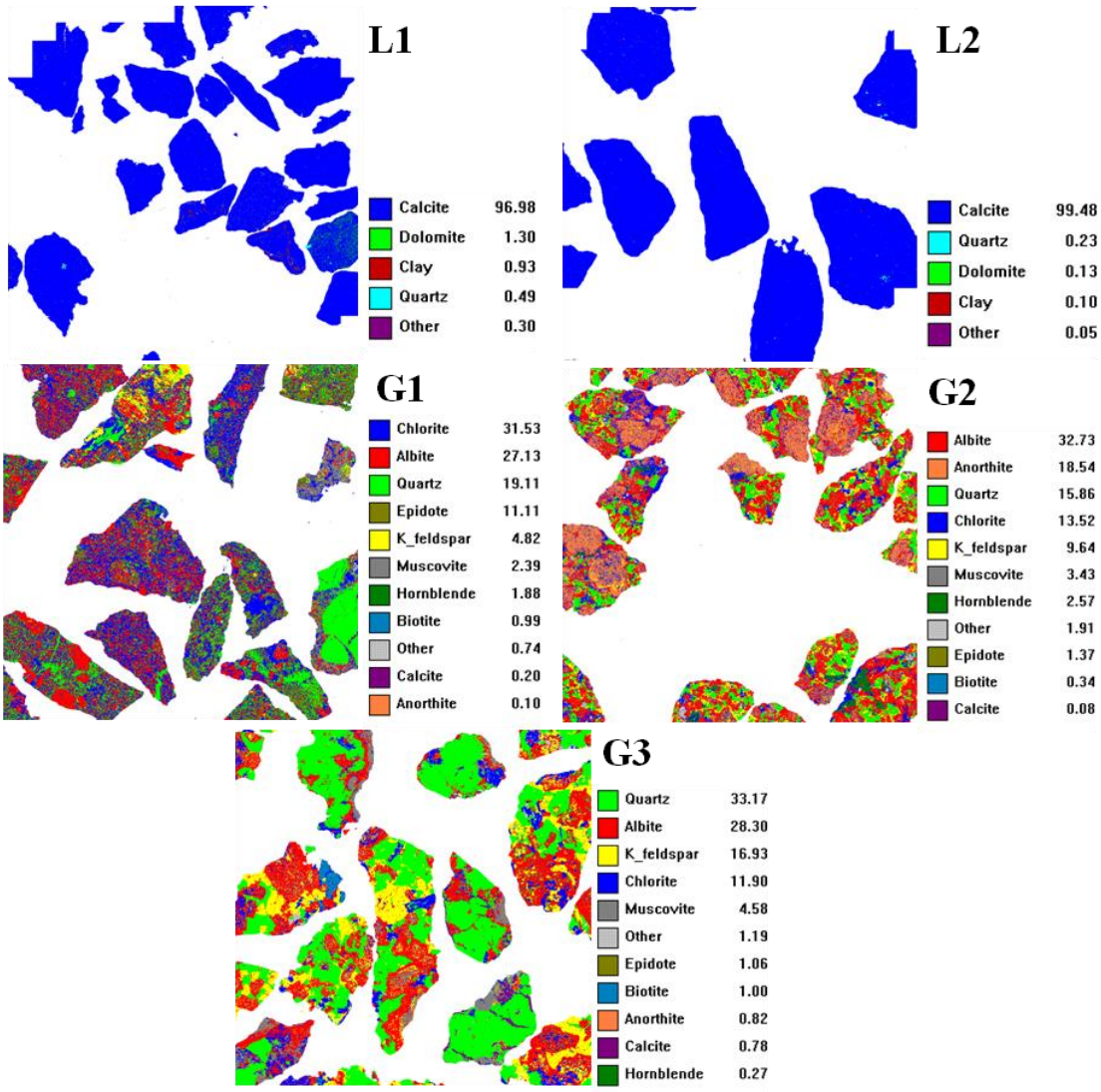

Figure 1. Mineral mosaic of five aggregates. L1 and L2 are classified as limestone while G1, G2 and G3 are granite

Figure 2. Aggregate substrate prepared from large boulders

Figure 3. Moisture conditioning of adhesion specimens

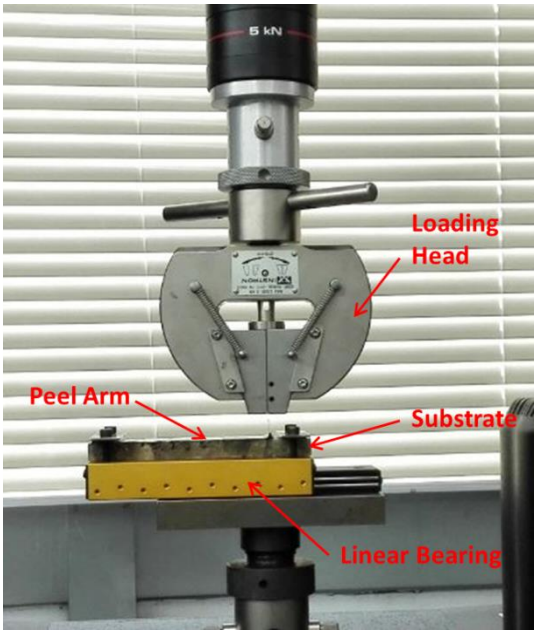

Figure 4. Details of peel test equipment

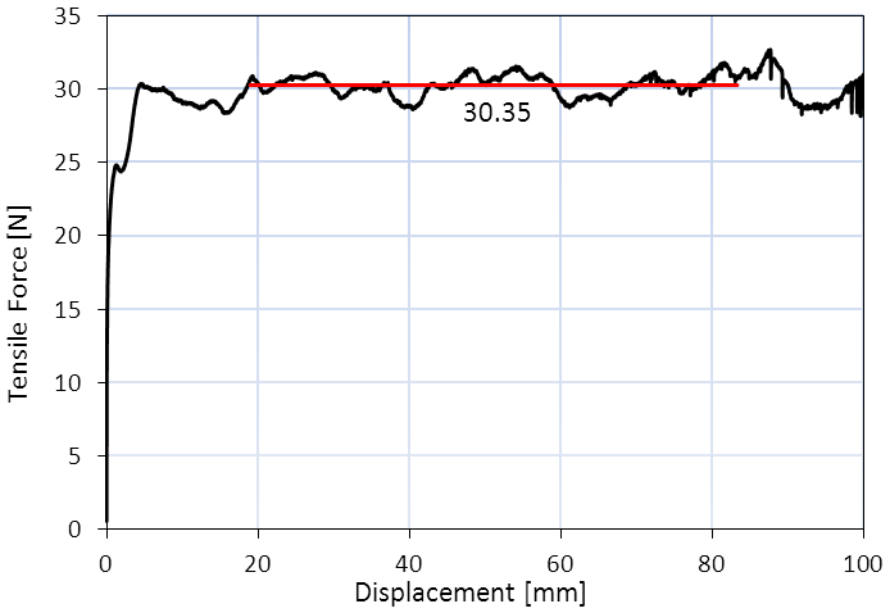

Figure 5. Measured tensile loading-displacement curve of B1-G1 in dry condition

Figure 6. Failure surface of specimens prepared with B1-G1 in dry condition

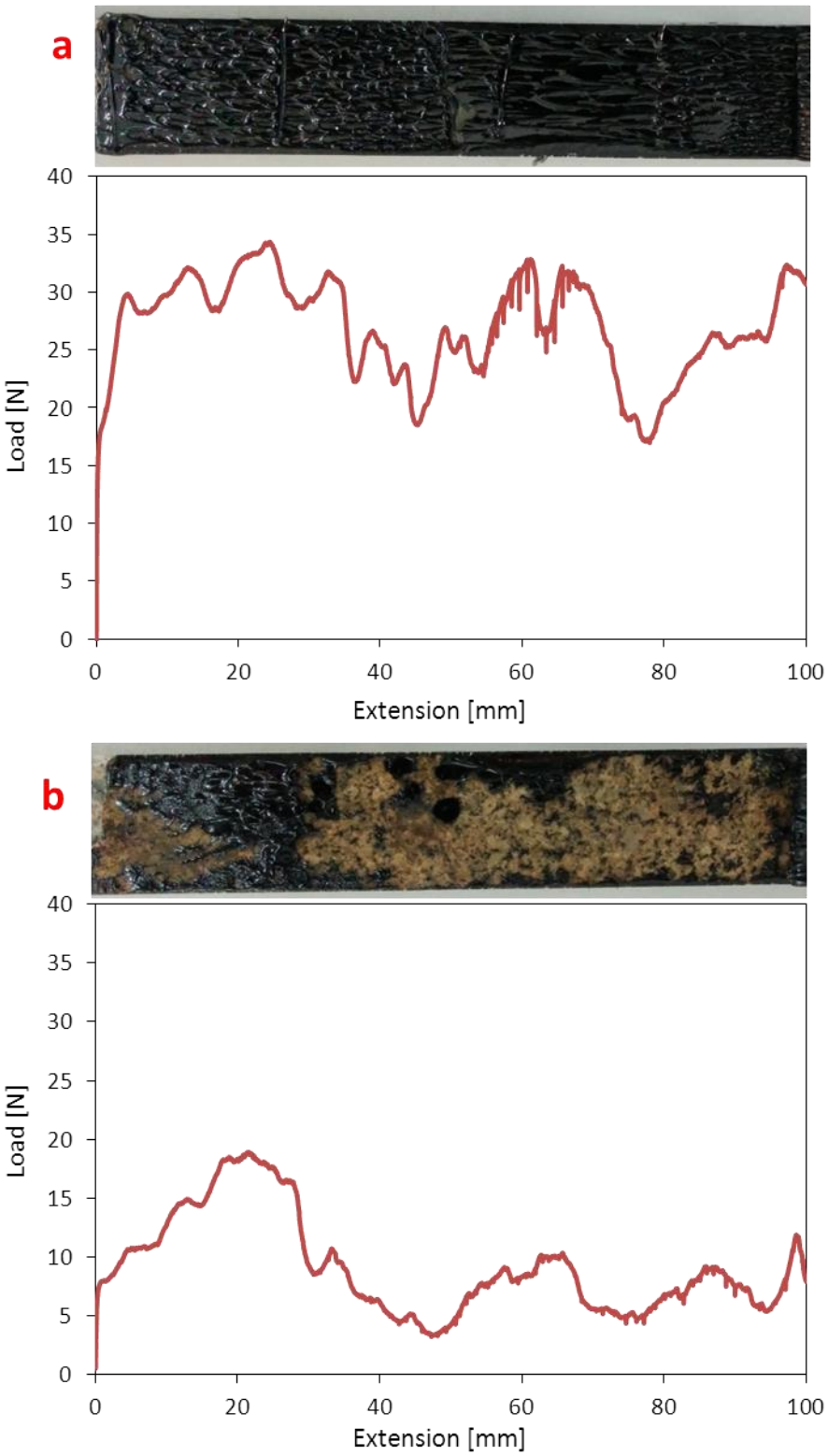

Figure 7. Failure surfaces and loading behaviour of two samples (B1-G1 and B1-G2) after 14 days of moisture conditioning using standard peel test

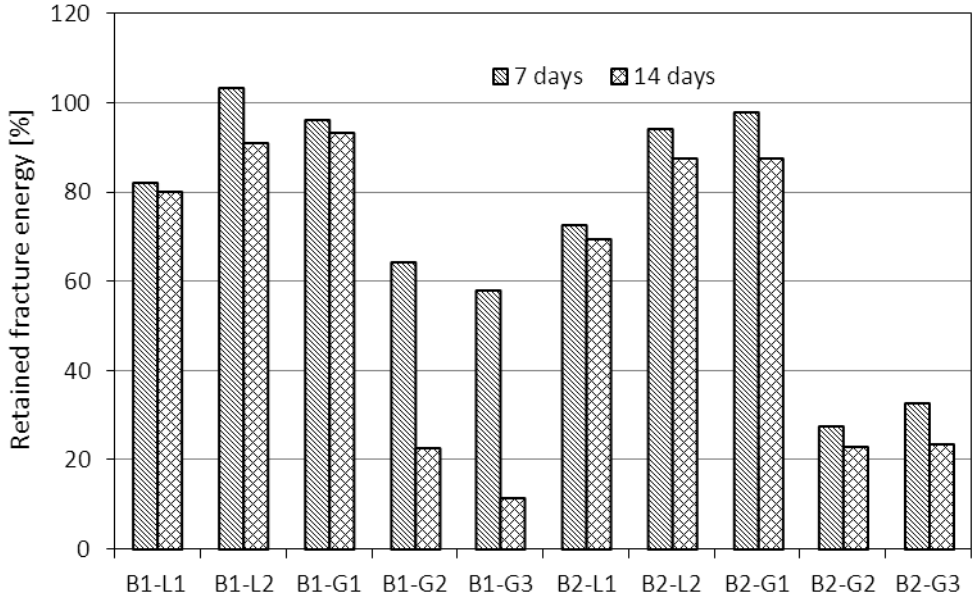

Figure 8. Retained fracture energy with respect to moisture damage achieved from peel test

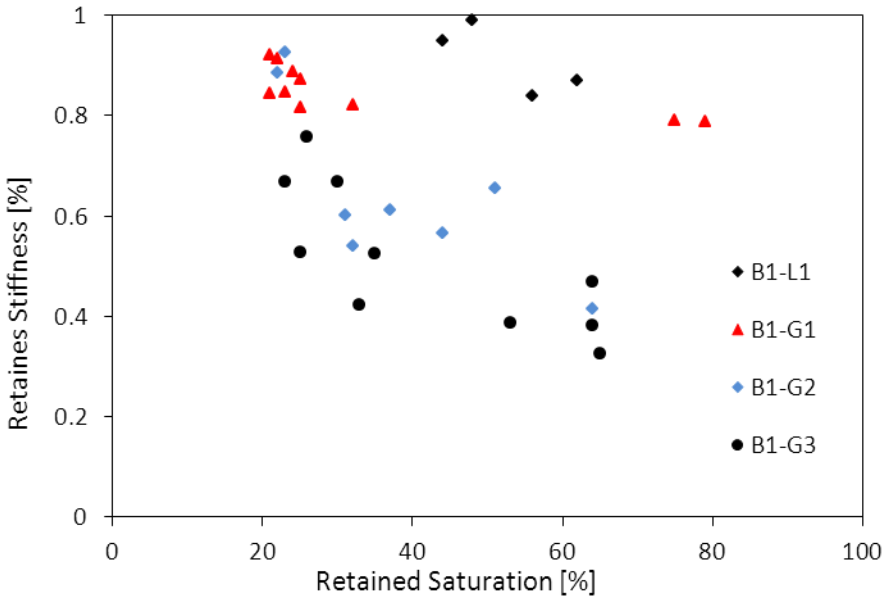

Figure 9. SATS retained stiffness results with retained saturation

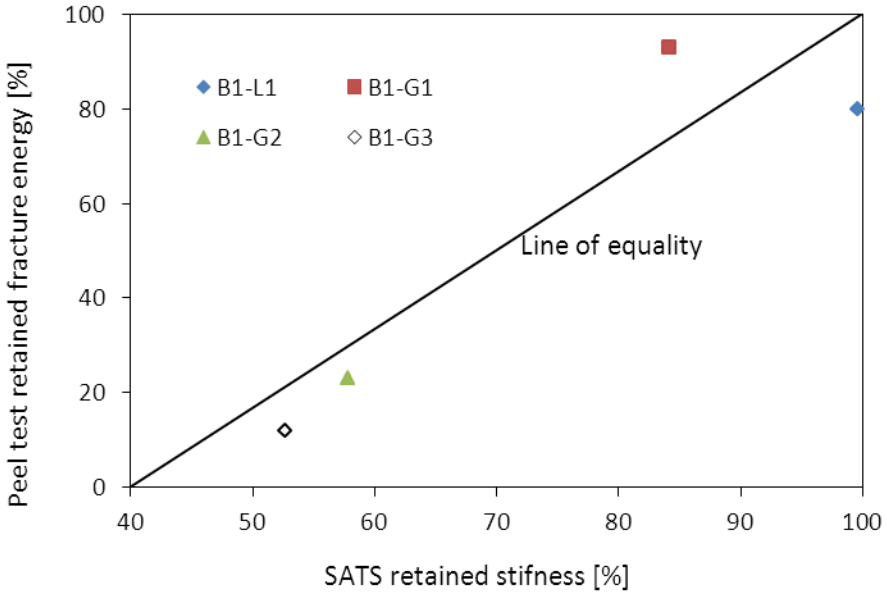

Figure 10. Plots of SATS retained stiffness and peel test retained fracture energy of specimens prepared with B1 bitumen showing good agreement between peel test and SATS results

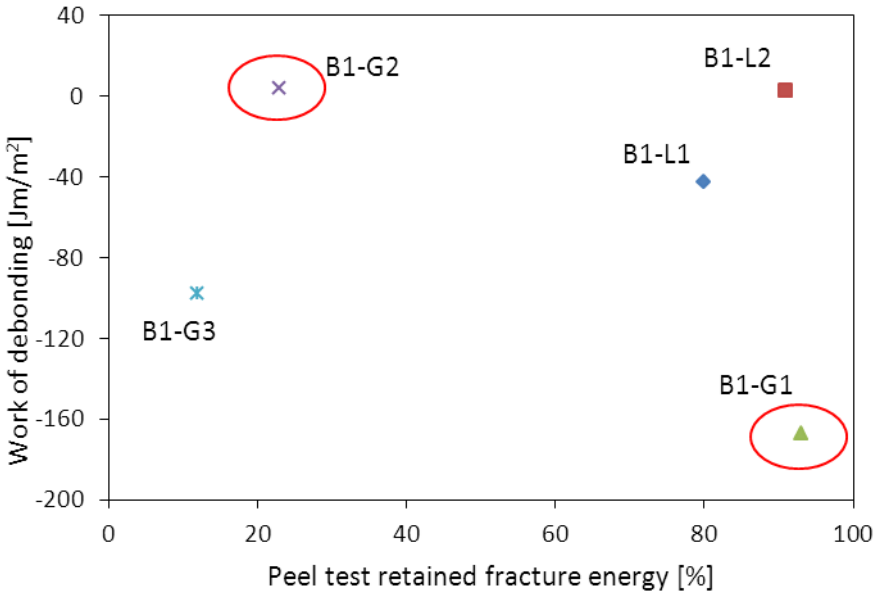

Figure 11. Plots of retained fracture energy and work of debonding. No clear relationship between intrinsic work of debonding and fracture energy from peel test.

Tables

Table 1. Water absorption of related aggregates

Aggregates	L1	L2	G1	G2	G3
Water absorption %	2.21	0.46	0.13	0.47	0.29

Table 2. Plastic bending parameters of the peel arm based on bi-linear model fit

Parameters	Quantity
Low strain modulus, E_1	58.2 GPa
High strain modulus, E_2	1.25 GPa
Yield strain, ε_y	0.046 %
α (E_2/E_1)	0.0215
Yield stress, σ_y	26.4 MPa

Table 3. Surface energy components of bitumen.

Bitumen	Surface energy components (mJ/m^2)			
	γ^{LW}	γ^+	γ^-	γ
B1	37.47	0.03	3.46	38.10
B2	32.94	0.06	2.07	33.62

Table 4. Surface energy components and SSA of aggregates

Aggregate	Surface energy components (mJ/m^2)				SSA (m^2/g)
	γ^{LW}	γ^+	γ^-	γ	
L1	75.3	108.9	49.7	222.4	0.1708
L2	82.2	6.7	59.3	122.0	0.0865
G1	69.1	17.3	568.3	267.5	0.3819
G2	68.3	16.4	40.8	120.0	0.3807
G3	68.0	163.9	122.7	351.6	0.4420

Table 5. Work of adhesion and cohesion in dry condition

Bitumen	W_{11} (mJ/m^2)	W_{12} (mJ/m^2)				
		L1	L2	G1	G2	G3
B1	76.19	147.42	123.22	125.28	118.39	152.30
B2	67.24	132.95	115.14	118.59	109.52	132.55

Note: W_{11} = work of cohesion for bitumen, W_{12} = work of adhesion for aggregate-bitumen combinations

Table 6. Work of debonding in wet condition

Bitumen	W_{131} (mJ/m^2)	W_{132} (mJ/m^2)				
		L1	L2	G1	G2	G3
B1	66.51	-42.26	2.59	-167.17	3.76	-97.93
B2	71.83	-49.58	1.66	-166.72	2.03	-106.38

Note: W_{131} = work of debonding of bitumen film in the presence of moisture, W_{132} = work of debonding at the aggregate-bitumen interface in the presence of moisture.

Table 7. Dry fracture energy (J/m^2) of aggregate-bitumen in the dry state at 20°C.

Bitumen	Mean ± 1SD (J/m^2)				
	L1	L2	G1	G2	G3
B1	988 ± 29.7	981 ± 29.4	1015 ± 6.4	1012 ± 16.5	999 ± 20.5
B2	480 ± 13.1	490 ± 13.6	494 ± 19.1	478 ± 21.4	486 ± 16.8

Note: B1 = 40/60 pen bitumen; B2 = 70/100 pen bitumen; L1 = limestone; L2 = limestone; G1= granite 1; G2 = granite 2; G3 = granite 3; SD = standard deviation